Capturing correlation in the spin frustrated H_3-ring using the generator coordinate method and spin-constrained generalized Hartree-Fock states

Xeno De Vriendt[a], John De Vos[a], Stijn De Baerdemacker[b], Patrick Bultinck[a], Guillaume Acke[a]

[a]Ghent Quantum Chemistry Group, Krijgslaan 281 (S3), B-9000 Ghent, Belgium; [b]Department of Chemistry, University of New Brunswick, 30 Dineen Drive, Fredericton, New Brunswick, E3B 5A3, Canada

ARTICLE HISTORY
Compiled September 20, 2022

Abstract
In spin frustrated H_3-rings, variationally minimal single Slater determinant descriptions break $\hat{S}^2$ and $\hat{S}_z$ symmetries in an effort to simultaneously minimize the interactions between all electrons. Given the underlying spin dynamics, it remains unclear how one can move beyond these symmetry-broken mean-field states and efficiently introduce electron correlation. Here we show that in frustrated systems the average longitudinal magnetization is a generator coordinate that is able to capture significant electron correlation. Our results demonstrate that tightly sampling the generator coordinate around spin phase transitions provides a good subspace for non-orthogonal configuration interaction. Combining these constrained generator coordinates with symmetry projection approaches could lead to efficient ansatzes that can incorporate complicated dynamics while maintaining symmetry quantum numbers.

KEYWORDS
spin frustration, generalized Hartree-Fock, constraints, Generator Coordinate Method, Non-Orthogonal Configuration Interaction

1. Introduction

In spin frustrated (sub)systems, the geometry of the (sub)system prevents the simultaneous minimization of the interactions between all sites, leading to unexpected physical properties [1, 2] (see fig. 1). To achieve the variationally minimal mean-field description of these competing magnetic interactions, each spin quantization axis should be allowed to rotate freely by breaking the $\hat{S}^2$ and $\hat{S}_z$ symmetries [3, 4]. As the underlying molecular spinors are then allowed to exist in a superposition of spin-up and spin-down states, the resulting states are no longer required to retain the correct symmetry of the exact solution [5], leading to symmetry-broken solutions. To reach results that are within chemical accuracy or to restore symmetries, one has to move beyond a strict mean-field approach by letting configurations interact [6].

When significant parts of the dynamics of the underlying physical processes can be expressed in terms of a so-called 'generalized coordinate', the Generator Coordinate

CONTACT Patrick Bultinck Email: patrick.bultinck@ugent.be
CONTACT Guillaume Acke Email: guillaume.acke@ugent.be

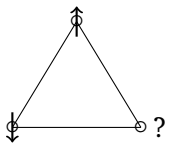

Figure 1. Visual representation of three sites arranged in an equilateral triangle with antiferromagnetic interactions between three spins, each of which is localized on one site. As the total energy is minimized when each spin is oppositely aligned with respect to its neighboring spins, the third spin is frustrated because it cannot simultaneously minimize its interactions with the other two spins.

Method (GCM) offers a tractable approach by constructing the many-body wavefunction as a linear superposition of (generally non-orthogonal) generator states that are labeled by the underlying collective (generator) coordinates and solving the equations of motion in the space spanned by those generator states [7–11]. Although the choice of the generator coordinate is essentially arbitrary, ideally the generator states should span a space that contains significant parts of the dynamics of the underlying physical processes [11]. For example, in Generator Coordinate Hartree-Fock (GCHF), one chooses the exponent of the underlying basis functions as a generator coordinate, leading to a collection of basis functions instead of a single basis function with a fitted optimal exponent [12, 13]. In another variant of the GCM, one can obtain explicitly correlated wave functions by constructing a systematic collection of compact wave functions with explicit dependence on the interelectronic separation [14]. In symmetry restoring approaches, a parametrized group of symmetry operators are applied on a symmetry broken (mean-field) reference such that one can recover the correct symmetries by diagonalizing the Hamiltonian in the (non-orthogonal) basis formed by the elements of the group [15–17]. In the general case of collective deformations (i.e. the ordered movement of many constituent parts of the system), the generator states are generated by constrained mean-field calculations [18–20]. In this way, the principal components of the deformation are controlled through the generator coordinate, while the other degrees of freedom are variationally minimized [11]. Note that the above strategies to create generator states can be mixed when dealing with several collective coordinates [10, 21, 22].

In the case of spin-frustrated systems, model Hamiltonians can guide us to parameters than can be used as generator coordinate across the phase transitions associated with spin frustration [23–25]. In the quantum 1D Ising model unrestricted Slater determinants are eigenfunctions [23], while adding a transverse magnetic field introduces correlations to excited states that are reflected in an increased transverse magnetization. Similarly, in the Heisenberg model a longitudinal magnetic field can break its spin-rotational invariance and lead to non-zero longitudinal magnetization [23]. In this study, we will show that the longitudinal magnetization is a generator coordinate that is able to capture much of the relevant physics of frustrated H_3-rings.

2. Theory

2.1. Generalized Hartree-Fock and spinors

In an orthonormal basis $\{\boldsymbol{\phi}_P(\mathbf{r}) \,|\, P = 1 \cdots M\}$ of M two-component spinors [26–29]

$$\boldsymbol{\phi}_P(\mathbf{r}) \mapsto \begin{pmatrix} \phi_P^\alpha(\mathbf{r}) \\ \phi_P^\beta(\mathbf{r}) \end{pmatrix}, \tag{1}$$

the usual elementary annihilation and creation operators $\hat{a}_P$ and $\hat{a}_P^\dagger$ obey the fermion anti-commutation relations [30–33]

$$[\hat{a}_P, \hat{a}_Q^\dagger]_+ = \delta_{PQ} \quad \text{and} \quad [\hat{a}_P^\dagger, \hat{a}_Q^\dagger]_+ = 0\,. \tag{2}$$

Note that in general the individual spinors in eq. (1) are not eigenvectors of the Pauli matrix σ_z. Hence, wave functions constructed with these elementary operators $\hat{a}_P$ and $\hat{a}_P^\dagger$ are symmetry-broken and not necessarily eigenvectors of total projected spin $\hat{S}_z$. When one of the spin-components of each spinor is zero, they are eigenvectors of σ_z (i.e. they are *spin-orbitals*), which leads to considerable simplifications in subsequent second quantized derivations [29].

The generalized Hartree-Fock wave function model can then be expressed as [34, 35]

$$|\text{GHF}(\boldsymbol{\kappa})\rangle = \exp(-\hat{\kappa}) \left(\prod_I \hat{a}_I^\dagger \right) |\text{vac}\rangle\,, \tag{3}$$

with $|\text{vac}\rangle$ the usual Fock vacuum, I a label for a set of orthonormal spinors that are 'occupied' in the single-Slater determinant and $\hat{\kappa}$ the anti-unitary generator of spinor rotations [6]

$$\hat{\kappa} = \sum_{PQ} \kappa_{PQ} \hat{a}_P^\dagger \hat{a}_Q \quad \text{with} \quad \boldsymbol{\kappa}^\dagger = -\boldsymbol{\kappa}\,. \tag{4}$$

In practice, each of the spinor components is expanded in a known scalar basis (usually an atomic orbital (AO) basis) of K (with $M = 2K$) basis functions $\{\varphi_\mu(\mathbf{r}) \,|\, \mu = 1 \cdots K\}$

$$\phi_P^\sigma(\mathbf{r}) = \sum_\mu \varphi_\mu(\mathbf{r}) C_{\mu P}^\sigma\,, \tag{5}$$

with $\mathbf{C}$ the expansion coefficient matrix and where we have used the label σ to designate either α or β. Optimization of the GHF wave function model with respect to the spinor expansion coefficients $\mathbf{C}$ leads to the GHF self-consistent field (SCF) equations

$$\mathbf{FC} = \mathbf{SC}\boldsymbol{\varepsilon}\,, \tag{6}$$

formulated in the AO basis. Here, the Fock matrix $\mathbf{F}$ has a (2×2) block matrix spin

structure of K by K blocks

$$\mathbf{F} = \begin{pmatrix} \mathbf{F}^{\alpha\alpha} & \mathbf{F}^{\alpha\beta} \\ \mathbf{F}^{\beta\alpha} & \mathbf{F}^{\beta\beta} \end{pmatrix}, \tag{7}$$

whose off-diagonal blocks consist of the off-diagonal core Hamiltonian and two-electron exchange contributions [26, 27]. In unrestricted Hartree-Fock (UHF) theory, the off-diagonal blocks are zero while in restricted Hartree-Fock (RHF) theory, the top-left ($\alpha\alpha$) and bottom-right ($\beta\beta$) blocks are also required to be equal.

When performing Hartree-Fock calculations, it may happen that the obtained solution is not an energy minimum within its own set of constraints (an internal instability) or there may be a lower energy solution if one breaks some specific symmetry (an external instability). As detailed by Stuber and Paldus [4], strictly negative eigenvalues in the Hartree-Fock Hessian $\mathbf{M}$

$$\mathbf{M} = \begin{pmatrix} \mathbf{A} & \mathbf{B} \\ \mathbf{B}^* & \mathbf{A}^* \end{pmatrix} \tag{8}$$

indicate an instability, and we can follow the eigenvector $\mathbf{J}$ corresponding to the lowest negative eigenvalue by exponentiating the mixing matrix $\mathbf{K}$

$$\mathbf{K} = \begin{pmatrix} \mathbf{0} & -\mathbf{J}^\dagger \\ \mathbf{J} & \mathbf{0} \end{pmatrix} \tag{9}$$

and applying the resulting unitary rotation to the expansion coefficients $\mathbf{C}$

$$\mathbf{C}' = \mathbf{C}e^{-s\mathbf{K}} \tag{10}$$

with s a small step in the direction $\mathbf{K}$ [5]. In contrast to RHF and UHF, where following external instabilities requires breaking symmetries, all instabilities in complex GHF are internal as this method has broken spin, time-reversal and complex conjugation symmetries.

2.2. Constraining wave function models

In general, a wave function model $|\Psi(\mathbf{p})\rangle$, parametrized by the model parameters $\mathbf{p}$, can be optimized by solving a particular set of equations

$$\mathbf{F}(\mathbf{p}^\star) = \mathbf{0}, \tag{11}$$

where $\mathbf{p}^\star$ denotes the optimal values of the model parameters. The optimized energy $\mathscr{E}$ is then found by evaluating the energy function associated to the model at these optimal parameters

$$\mathscr{E} = E(\mathbf{p}^\star). \tag{12}$$

A feature m is then defined as a function of the optimal parameters

$$m(\mathbf{p}^\star) = M, \tag{13}$$

where M is the value of the feature m that is attained by the optimal model parameters.

In order to constrain the model parameters $\mathbf{p}^\star$ such that a target value M for the feature m is attained, we introduce the following Lagrangian

$$\mathscr{L}(\mathbf{p},\mu) = E(\mathbf{p}) - \mu(m(\mathbf{p}) - M)\,, \tag{14}$$

where the stationary condition for the Lagrange multiplier μ yields the original feature constraint

$$\left.\frac{\partial \mathscr{L}(\mathbf{p},\mu)}{\partial \mu}\right|_{\mu^\star,\mathbf{p}^\star} = -(m(\mathbf{p}^\star) - M) = 0 \Rightarrow m(\mathbf{p}^\star) = M\,, \tag{15}$$

and the stationary condition for the model parameters $\mathbf{p}$ can be written as

$$\left.\frac{\partial \mathscr{L}(\mathbf{p},\mu)}{\partial p_i}\right|_{\mu^\star,\mathbf{p}^\star} = \left.\frac{\partial E(\mathbf{p})}{\partial p_i}\right|_{\mathbf{p}^\star} - \mu^\star\left(\left.\frac{\partial m(\mathbf{p})}{\partial p_i}\right|_{\mathbf{p}^\star}\right) = 0\,. \tag{16}$$

The optimal energy $\mathscr{E}$ may then be found by evaluating the Lagrangian at the solution $(\mu^\star,\mathbf{p}^\star)$

$$\mathscr{L}(\mathbf{p}^\star,\mu^\star) = E(\mathbf{p}^\star) = \mathscr{E}\,. \tag{17}$$

Although, in general, any function of the model parameters $\mathbf{p}$ can be used as a feature [36–38], in this study we will only use the expectation value of $\hat{S}_z$

$$m(\mathbf{p}) = \frac{\langle\Psi(\mathbf{p})|\hat{S}_z|\Psi(\mathbf{p})\rangle}{\langle\Psi(\mathbf{p})|\Psi(\mathbf{p})\rangle}\,. \tag{18}$$

2.3. Generator Coordinate Method

In the Generator Coordinate Method, the wavefunction ansatz has the form

$$|\Psi\rangle = \int da\, f(a)\,|\Phi(a)\rangle\,, \tag{19}$$

where the generator states $|\Phi(a)\rangle$ depend on the generator coordinate a [8, 9]. The weight functions $f(a)$ can be determined by requiring that the expected energies are stationary

$$\delta\left(\frac{\langle\Psi|\hat{H}|\Psi\rangle}{\langle\Psi|\Psi\rangle}\right) = 0\,, \tag{20}$$

leading to the Hill-Wheeler integral equations [7]

$$\int da'\left[\mathscr{H}(a,a') - E\mathscr{S}(a,a')\right] f(a') = 0\,, \tag{21}$$

with

$$\mathscr{H}(a,a') = \left\langle \Phi(a) \middle| \hat{H} \middle| \Phi(a') \right\rangle \tag{22}$$

$$\mathscr{S}(a,a') = \left\langle \Phi(a) \middle| \Phi(a') \right\rangle . \tag{23}$$

In practice, the generator states are only sampled for a discrete set of values $\{a_i\}$, which transforms the kernel equation above into a generalized eigenvalue problem

$$\mathbf{HF} = E\mathbf{SF}, \tag{24}$$

with $\mathbf{F}$ the coefficients associated with the generator states and $\mathbf{S}$ the overlap matrix of the generator states. As $\mathbf{S}$ is not necessarily diagonal, this is formally equivalent to non-orthogonal configuration interaction (NOCI) in the generated states [39–44].

3. Methodology

As an equilateral H_3-ring is a prime example of a geometrically frustrated system, we will examine a neutral equilateral H_3-ring, which is stretched symmetrically during the dissociation process. Along the dissociation profile the single Slater determinant variational minimum is given by real valued GHF states which can be obtained by following any instabilities until the solution is stable.

By imposing an average $\langle \hat{S}_z \rangle$, we can obtain the single Slater determinant variational minimum by following the instabilities of the associated Lagrangian, leading to the associated Constrained Generalized Hartree-Fock (CGHF) state. As obtaining such constrained states along the entire dissociation profile can be computationally challenging, we will use small basis sets for this proof-of-principle (STO-3G and 6-31G).

The resulting symmetry broken constrained states are then used as generator states in the associated NOCI, with the aim of capturing as much correlation as possible with as few generator states as possible. As the GCM is also a wavefunction model, we will also impose average constraints on the ground state of this model by a similar Lagrangian approach in order to approximate the symmetry in the mean.

We will benchmark our results against FCI results and NOCI calculations in a symmetry adapted basis that is constructed by acting the $\hat{C}_3^1$ and $\hat{C}_3^2$ operators on a UHF single slater determinant. Such a symmetry adapted basis consists of three (or six if we include the α/β flipped states) basis states and has already been shown to capture static correlation [16, 45].

All methods were implemented in the Ghent Quantum Chemistry Package [29].

4. Results

Imposing different $\langle \hat{S}_z \rangle$-constraints on the mean-field yields distinct energetic states, where the $\langle \hat{S}_z \rangle = 0.5$ au and $\langle \hat{S}_z \rangle = 1.5$ au CGHF states coincide with their respective UHF $S_z = 0.5$ and $S_z = 1.5$ states (see fig. 2). As the CGHF potential energy surfaces smoothly deform as a function of $\langle \hat{S}_z \rangle$, $\langle \hat{S}_z \rangle$ provides a continuous generator coordinate which supports the deformation of the spin projection. We note that none of the CGHF states is bound and that each CGHF state is higher in energy than the unconstrained GHF $\langle \hat{S}_z \rangle = 0$ state.

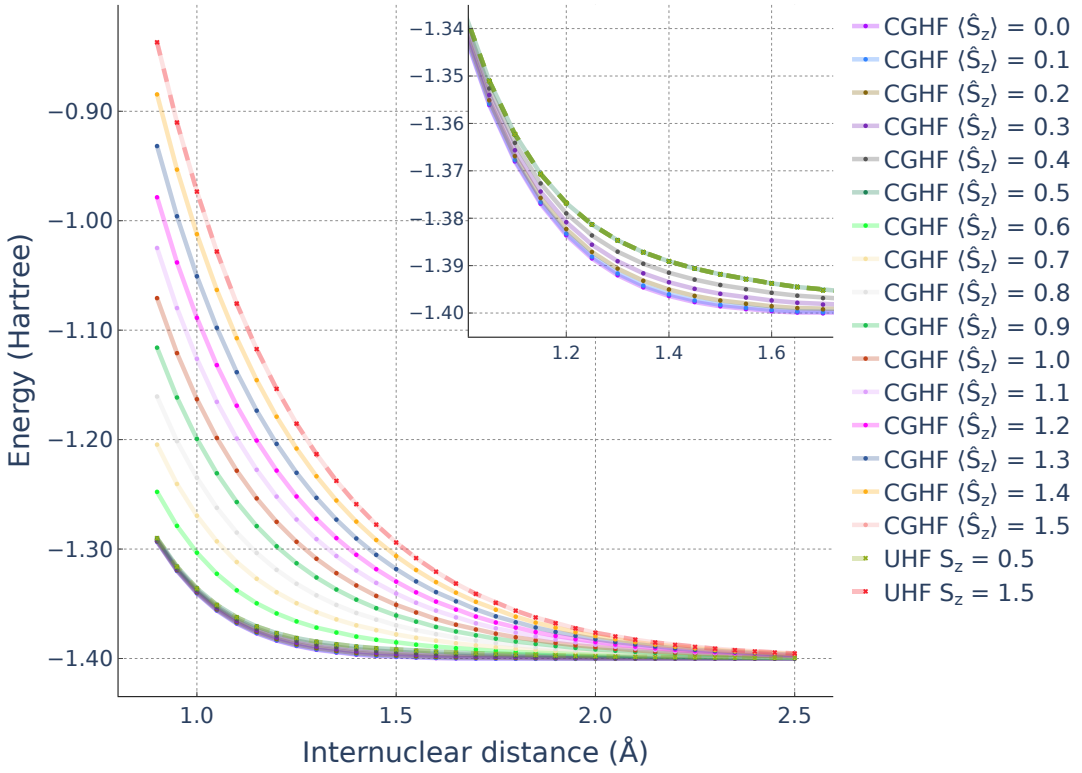

Figure 2. Potential energy surfaces for CGHF states in the minimal STO-3G basis set constrained to $\langle \hat{S}_z \rangle$'s in the range of 0.0 au to 1.5 au in steps of 0.1 au. The CGHF states are contrasted with the two UHF states with $S_z = 0.5$ au and $S_z = 1.5$ au.

Given that this generator coordinate supports a smooth deformation in $\langle \hat{S}_z \rangle$ for GHF states, we need to sample this coordinate (see eq. (24)) in such a way that only those generator states that are the most pertinent for the dynamics at hand are included in the associated NOCI. As can be seen in fig. 2, the CGHF states constrained *below* the spin-frustrated UHF $S_z = 0.5$ solution are qualitatively different from those constrained above, with a marked discontinuity in the energy as a function of $\langle \hat{S}_z \rangle$ at intermediate bonding distances (see fig. 3). Whereas the UHF($S_z = 0.5$) state has two

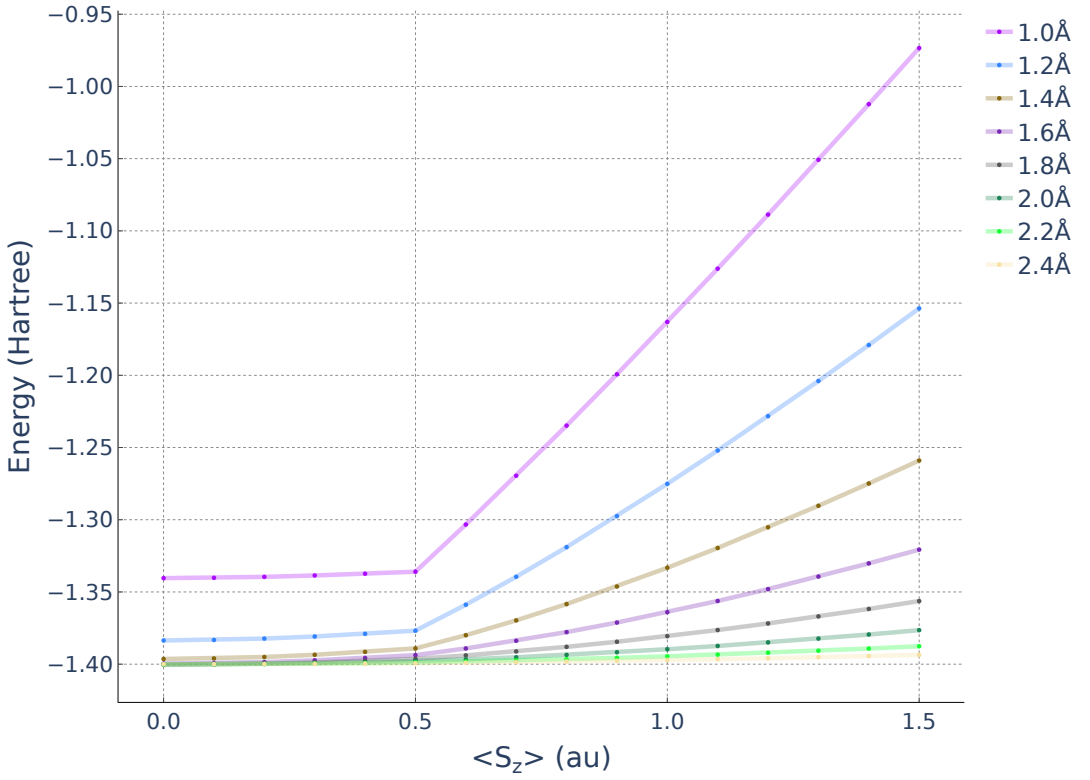

Figure 3. Energy of the CGHF states in the minimal STO-3G basis set as a function of $\langle \hat{S}_z \rangle$ for a range of internuclear distances.

occupied α-orbitals and one occupied β-orbital, one spinor of the CGHF($\langle \hat{S}_z \rangle = 0.4$) state gains contributions in its β components (see fig.S.1). On the other hand, when transitioning to CGHF($\langle \hat{S}_z \rangle = 0.6$), a different spinor gains α components. As the respective constraints are lowered towards $\langle \hat{S}_z \rangle = 0.0$ or increased towards $\langle \hat{S}_z \rangle = 1.0$, these components gradually increase, but the changes remain more or less contained within the same spinors. As these two behaviors represent two different modes of excitation, these results indicate that we should sample the generator states symmetrically around $\langle \hat{S}_z \rangle$.

In order to find the most economical basis in which NOCI calculations can already capture most of the electron correlation, we vary the number of states and the distance at which we sample (0.1 au or "wide" sampling versus 0.01 or "tight" sampling). Although none of the underlying generator states exhibit a bound state (fig. 2), all NOCI's that mix these states lead to bound state dissociation profiles (see fig. 4). In contrast to the nine states required by FCI, a tightly sampled basis consisting of five

generator states already captures much of the correlation energy. When using widely

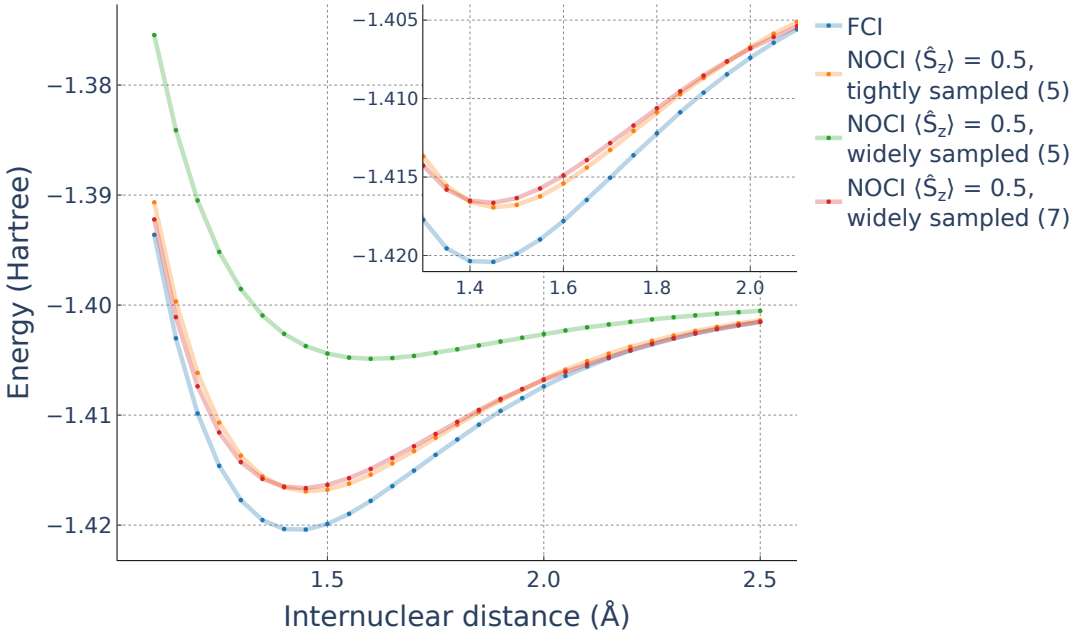

Figure 4. Potential energy surfaces of constrained NOCI calculations in the STO-3G basis set in a tightly sampled subspace compared to differently sized widely sampled subspaces and FCI.

sampled basis states, seven such generator states are required to achieve similar performance to the tightly sampled basis, with a markedly worse performance when only five states are used. Based on these results we surmise that by sampling closely to the spin-phase transition, we are effectively sampling states that have approximately the same energy, but have very different configurations and are as such ideally suited for capturing correlation.

Although a NOCI in the proposed CGHF basis adequately captures dynamic correlation in the STO-3G basis, the three-dimensional spatial symmetry adapted UHF basis is better suited for capturing static correlation (fig. 5). If we include states that have their spins flipped, we improve further on the CGHF-NOCI performance at the cost of one additional basis state. In contrast, in the 6-31G basis the NOCI PES calculated in either basis of spatial symmetry adapted UHF states is unable to adequately mimic the FCI dissociation profile and only provides a small energetic correction to CGHF-NOCI (fig. 6). While CGHF-NOCI is unable to account for a considerable amount of dynamic electron correlation, it does give a balanced description of the dissociation process in a space of only five basis states instead of the ninety states required by FCI. These results indicate that by sampling the generator coordinate closely to spin-phase transitions, we can generate small subspaces in which the associated NOCI is able to capture significant electron correlation.

As recently shown by Frosini et al. in the context of nuclei [46], constrained generator states can be combined with a (perturbative) symmetry restoring approach, leading to an efficient multi-reference many-body perturbation theory. In subsequent work we will determine to what extent this approach is generally applicable within electronic structure and what correlations can be captured with local constraints.

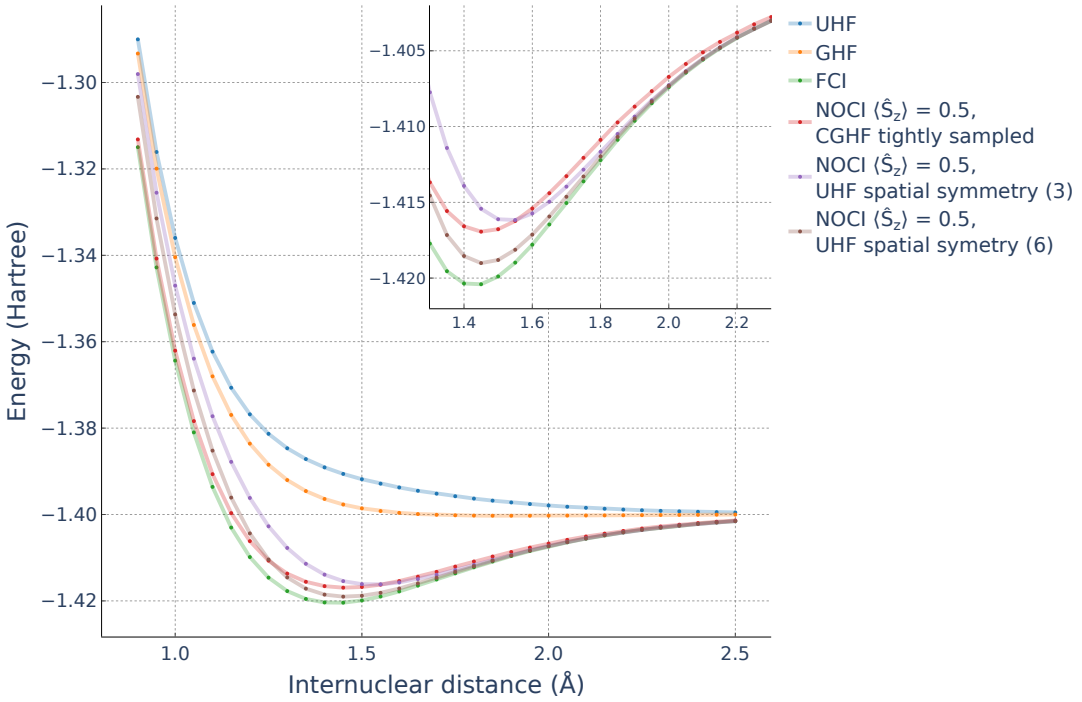

Figure 5. Potential energy surfaces of constrained NOCI calculations in the minimal STO-3G basis set for a CGHF basis (0.48 au to 0.52 au (tightly sampled)) and two different symmetry adapted UHF subspaces compared to UHF, GHF and FCI.

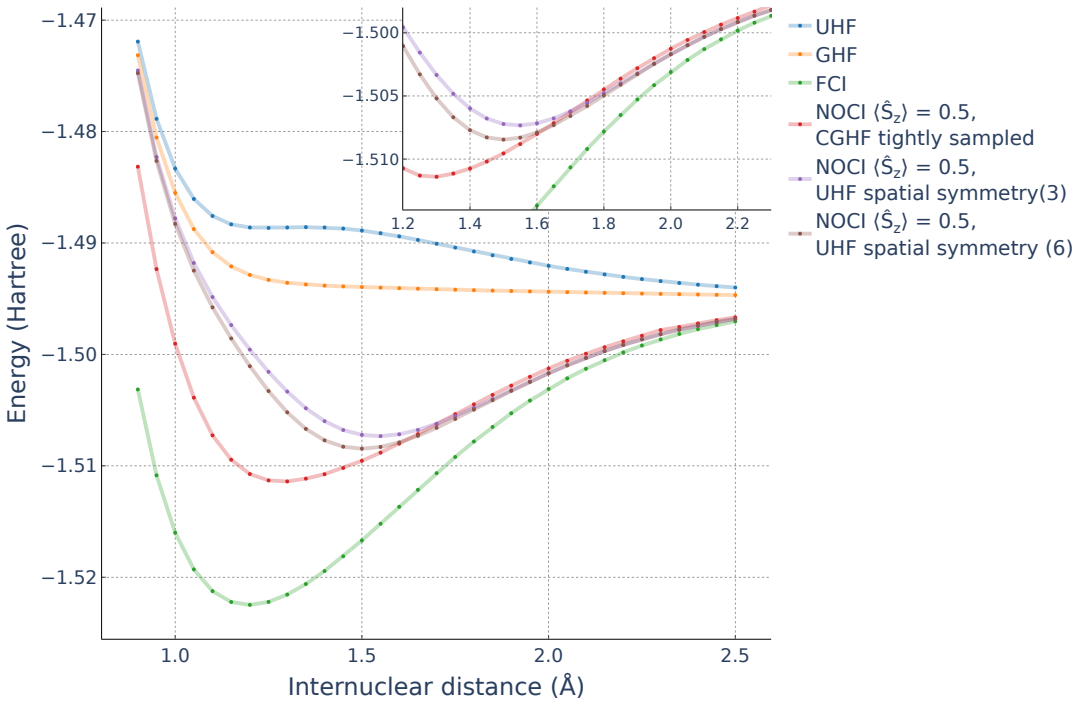

Figure 6. Potential energy surfaces of constrained NOCI calculations in the 6-31G basis set for a CGHF basis (0.48 au to 0.52 au (tightly sampled)) and two different symmetry adapted UHF subspaces compared to UHF, GHF and FCI.

5. Conclusions

In this work, we have shown that in spin frustrated H_3-rings we can recover significant electron correlation by tightly sampling the average longitudinal magnetization as a generator coordinate and mixing the concomitant generator states in a non-orthogonal configuration interaction. Our study indicates that constrained states can provide efficient bases if the constraint is associated with the the dynamics that govern the chemistry of the system. In subsequent work we will determine to what extent this approach is generally applicable within electronic structure and what correlations can be captured when combining this methodology with symmetry projections.

Acknowledgements

Parts of this research were funded by FWO research project G031820N, the Canada Research Chairs Program (SDB) and the New Brunswick Innovation Foundation. The computational resources (Stevin Supercomputer Infrastructure) and services used in this work were provided by the VSC (Flemish Supercomputer Center), funded by Ghent University, FWO and the Flemish Government - department EWI.

References

[1] M. Harris, Nature **456** (7224), 886–887 (2008).
[2] L. Balents, Nature **464** (7286), 199–208 (2010).
[3] P. Lykos and G. Pratt, Rev. Mod. Phys. **35** (3), 496 (1963).
[4] J.L. Stuber and J. Paldus, Fundamental world of quantum chemistry: A tribute volume to the memory of Per-Olov Löwdin **1**, 67–139 (2003).
[5] J.J. Goings, F. Ding, M.J. Frisch and X. Li, J. Chem. Phys. **142** (15), 154109 (2015).
[6] T. Helgaker, P. Jorgensen and J. Olsen, *Molecular electronic-structure theory* (, , 2014).
[7] J.J. Griffin and J.A. Wheeler, Phys. Rev. **108** (2), 311 (1957).
[8] J.P. Blaizot and G. Ripka, *Quantum theory of finite systems* (, , 1986).
[9] P. Ring and P. Schuck, *The nuclear many-body problem* (, , 2004).
[10] J.A. Sheikh, J. Dobaczewski, P. Ring, L.M. Robledo and C. Yannouleas, J. Phys. G: Nucl. Part. Phys. **48** (12), 123001 (2021).
[11] M. Verriere and D. Regnier, Front. Phys. **8**, 233 (2020).
[12] F. Arickx, J. Broeckhove, E. Deumens and P. Van Leuven, J. Comput. Phys. **39** (2), 272–281 (1981).
[13] M. Trsic and A. Da Silva, *Electronic, atomic and molecular calculations: applying the generator coordinate method* (, , 2011).
[14] A.J. Thakkar and V.H. Smith Jr, Phys. Rev. A **15** (1), 1 (1977).
[15] G.E. Scuseria, C.A. Jiménez-Hoyos, T.M. Henderson, K. Samanta and J.K. Ellis, J. Chem. Phys. **135** (12), 124108 (2011).
[16] C.A. Jiménez-Hoyos, T.M. Henderson, T. Tsuchimochi and G.E. Scuseria, J. Chem. Phys. **136** (16), 164109 (2012).
[17] Y. Cui, I.W. Bulik, C.A. Jiménez-Hoyos, T.M. Henderson and G.E. Scuseria, J. Chem. Phys. **139** (15), 154107 (2013).
[18] M. Baranger, Phys. Rev. **122** (3), 992 (1961).
[19] P. Bonche, J. Dobaczewski, H. Flocard, P.H. Heenen and J. Meyer, Nucl. Phys. A **510** (3), 466–502 (1990).
[20] K. Tanabe and M. Ogoshi, J. Phys. Soc. Japan **59** (9), 3307–3321 (1990).
[21] M. Bender, P.H. Heenen and P.G. Reinhard, Rev. Mod. Phys. **75** (1), 121 (2003).

[22] M. Bender, P. Bonche and P.H. Heenen, Phys. Rev. C **74** (2), 024312 (2006).
[23] B. Powell, arXiv preprint arXiv:0906.1640 (2009).
[24] H. Nishimori and G. Ortiz, *Elements of phase transitions and critical phenomena* (, , 2010).
[25] S. Sachdev, *Quantum phase transitions* (, , 2011).
[26] S. Sen and E.I. Tellgren, J. Chem. Phys. **148** (18), 184112 (2018).
[27] S. Sun, D.B. Williams-Young, T.F. Stetina and X. Li, J. Chem. Theory Comput. **15** (1), 348–356 (2019).
[28] C. Cohen-Tannoudji, B. Diu and F. Laloë, *Quantum Mechanics, Volume 2: Angular Momentum, Spin, and Approximation Methods* (Wiley-VCH Verlag GmbH & Co. KGaA, Weinheim, Germany, 2020).
[29] L. Lemmens, X. De Vriendt, D. Tolstykh, T. Huysentruyt, P. Bultinck and G. Acke, J. Chem. Phys. **155** (8), 084802 (2021).
[30] P.R. Surján, *Second Quantized Approach to Quantum Chemistry, An Elementary Introduction* (Springer-Verlag, Berlin, Germany, 1989).
[31] T. Helgaker and P. Jørgensen, J. Chem. Phys. **95** (4), 2595–2601 (1991).
[32] T. Helgaker, S. Coriani, P. Jørgensen, K. Kristensen, J. Olsen and K. Ruud, Chem. Rev. **112** (1), 543–631 (2012).
[33] C. Cohen-Tannoudji, B. Diu and F. Laloë, *Quantum Mechanics, Volume 3: Fermions, Bosons, Photons, Correlations, and Entanglement* (Wiley-VCH Verlag GmbH & Co. KGaA, Weinheim, Germany, 2020).
[34] H. Fukutome, Int. J. Quantum Chem. **20** (5), 955–1065 (1981).
[35] P.O. Löwdin and I. Mayer, Adv. Quantum Chem. **24**, 79–114 (1992).
[36] X. De Vriendt, L. Lemmens, S. De Baerdemacker, P. Bultinck and G. Acke, J. Chem. Theory Comput. **17** (11), 6808–6818 (2021).
[37] X. De Vriendt, D. Van Hende, S. De Baerdemacker, P. Bultinck and G. Acke, J. Chem. Phys. **156** (24) 244115 (2022)
[38] L. Lemmens, X. De Vriendt, P. Bultinck and G. Acke, J. Chem. Theory Comput. (2022).
[39] P.Å. Malmqvist, Int. J. Quantum Chem. **30** (4), 479–494 (1986).
[40] P.Y. Ayala and H.B. Schlegel, J. Chem. Phys. **108** (18), 7560–7567 (1998).
[41] A.J. Thom and M. Head-Gordon, J. Chem. Phys. **131** (12), 124113 (2009).
[42] N.J. Mayhall, P.R. Horn, E.J. Sundstrom and M. Head-Gordon, Phys. Chem. Chem. Phys. **16** (41), 22694–22705 (2014).
[43] E.J. Sundstrom and M. Head-Gordon, J. Chem. Phys. **140** (11), 114103 (2014).
[44] J. Olsen, J. Chem. Phys. **143** (11), 114102 (2015).
[45] B. C. Huynh and A. J. W. Thom, J. Chem. Theory Comput. **16** (2), 904–930 (2019).
[46] M. Frosini, T. Duguet, J.-P. Ebran, V. Soma, Eur. Phys. J. A **58** (62) (2022)